

# An Experimental Model For Sonar Sensors

Jaime Fonseca, Júlio S. Martins and Carlos Couto

*Dept. of Industrial Electronics, University of Minho, Guimarães, Portugal*

*[Jaime@dei.uminho.pt](mailto:Jaime@dei.uminho.pt), [jmartins@dei.uminho.pt](mailto:jmartins@dei.uminho.pt) and [ccouto@dei.uminho.pt](mailto:ccouto@dei.uminho.pt)*

## Abstract

*This paper describes an empirical model of the time-of-flight of a sonar sensor, derived from data collected with a Polaroid ultrasonic range finder. The goal of this model is to enable the acquisition of the profile of surfaces with a minimum error. These surfaces can present regions with different depths, corners and specular surfaces. To minimize the constraints of sonar sensors some software and hardware options are described and an empirical model obtained from real time data is presented. This model is based in two proposed concepts: Points of Constant Depth (PCD) and Areas of Constant Depth (ACD).*

## 1. Introduction

To widen the range of applications of robotic devices, both in industry and research, it is necessary to develop systems with high levels of autonomy and able to operate in unstructured environments with little *a priori* information. To achieve this degree of independence, the robot system must have an understanding of its surroundings, by acquiring and manipulating a model of its environment. For that purpose, it needs a variety of sensors to be able to interact with the real world and mechanisms to extract meaningful information from the data being provided.

The main need for manipulators and for mobile robots is the ability to acquire and handle information about the presence and localization of objects and empty spaces in the scope of the device. This is extremely important for fundamental operations that involve spatial and geometric reasoning. Typically, due to limitations intrinsic to any kind of sensor, it is important to compose information coming from multiple readings, and build a coherent world-model.

Initially, ultrasonic sensors were heralded as a cheap solution to mobile robots for map building, localization, and navigation, because it provides direct range information at low cost. Sonar time-of-flight can measure distances with a high degree of accuracy. However, time-of-flight readings can be hard to interpret. Many

researchers have made the following comments on this subject [4]:

1. Ultrasonic sensors offer many shortcomings ... a) poor directionality that limits the accuracy in the determination of the spatial position on an edge to 10-50 cm, depending on the distance to the obstacle and the angle between the obstacle surface and the acoustic beam b) Frequent misreading ... c) Specular reflections that occur when the angle between the wave front and the normal to a smooth surface is too large.
2. Ultrasonic range data are seriously corrupted by reflections and specularities.
3. ... the use of a sonar range finder represents, in some sense, a worst case scenario for localization with range data ... .

The general conclusion of these works is that sonar is plagued by two problems: beam opening angle, what implies a poor angular resolution and specularity. However, in spite of these conclusions, ultrasonic sensors present several advantages, in addition to their low, cost which incentives its use:

1. Ultrasonic technology is known and dominated for a long time;
2. It doesn't present any risk for the safety of humans;
3. They are relatively easy to control;

For the purpose of the work here described, a PUMA 560 manipulator was equipped with a CCD video camera and four ultrasonic sensors on the wrist, to acquire data for internally representation of the geometry of the part's surface, exploiting the mobility of the robot. The camera defines the work area while the ultrasonic sensors enable the acquisition of the surface profile.

In this paper an experimental model for ultrasonic sensors will be presented. This model is based on numerical real time data and enables the acquisition of the surface profile with minimum error. In the Figure 1 are shown examples of some objects used to test the sensorial system implemented. The profile of these objects present corners, small depth differences between two or more regions in the surface. It is also possible that the object

has a specular surface-making very hard the acquisition of the surface profile by the ultrasonic sensors.

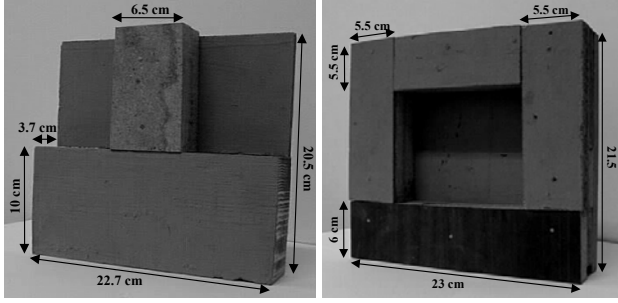


Figure 1. Examples the objects for acquire

The paper is organized as follows: section 2 describes the principles of the ultrasonic sensors; the section 3 present some models for the sonars; the section 4 present the implementation and results; the last section are the conclusions.

## 2. Ultrasonic sensors principles

The basic principle of a distance measurement using a ultrasonic sensor is the evaluation of the time-of-flight (TOF), which is the time interval between the emission of the transmission wave and the reception of its echo. In the present case, the sonar sensor is a Polaroid Ultrasonic range finder, which measures TOF with a single transducer that acts both as transmitter and receiver, with a blanking time between the two situations (Figure 2).

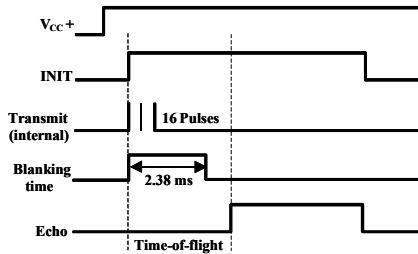


Figure 2. Example of a single echo mode cycle without blanking input

The TOF value corresponds to the double of the distance between the transmitter and the reflective surface, given by:

$$d = \frac{1}{2} \times c \times TOF$$

$$\text{where, } c = 331.4 \sqrt{\frac{T + 273}{273}} \text{ m/s.}$$

$T$  is the environment temperature in degrees Centigrade and  $c$  is the sound speed in the air

It is easily seen from this relationship that the sound speed is greatly affected by the temperature. If accurate values of the distance are desired then the temperature values must be known. However, the major acoustical factors affecting the performance of a sonar ranging

system are related to the transducer performance, operating frequency, and the desired maximum range. Neglecting the function of the electronics, and if there are no large variations in pressure and temperature, there is one main relationship to deal with: the relationship between transducer size, beamwidth, and operating frequency [2].

To analyze transducer radiation characteristics, the transducer can be treated as a plane circular piston set in an infinite baffle. Its radiation characteristic function then is given by:

$$P(\theta) = \frac{2 J_1(ka \sin(\theta))}{ka \sin(\theta)}$$

$$\text{where } k = \frac{2\pi}{\lambda} = 2\pi \frac{f}{c},$$

$a$  is the piston radius,  $\theta$  is the azimuthal angle and  $J_1$  is a Bessel function and  $\lambda$  is the wavelength.

It is interesting that the radiation pattern beamwidth comes as a function of frequency and transducer size. The beamwidth is most commonly expressed as the angle defined by the points around the principal axis where the radiation pattern is 3dB less than the value on the axis ( $\theta = 0$ ).

Therefore it is possible to set

$$\frac{2J_1(x)}{x} = -3dB = \frac{1}{\sqrt{2}}$$

To solve this relationship exactly requires an interactive procedure; however, a very good approximation can be achieved by expansion of the Bessel function to only 3 terms.

Expanding and solving yields

$$x = 1.62, \text{ where } x = ka \sin(\theta)$$

Therefore

$$\theta = \sin^{-1}\left(\frac{x}{ka}\right) = \sin^{-1}\left(\frac{1.62}{ka}\right) = \sin^{-1}\left(\frac{1.62\lambda}{2\pi a}\right) = \sin^{-1}\left(\frac{1.62c}{2\pi fa}\right)$$

The beamwidth is  $2\theta$ . A plot of beamwidth versus frequency and transducer radius is shown in Figure 3. This graph provides an easy method given any two parameters to find the third, or given a desired beamwidth to see the appropriate combinations of transducer size and operating frequency.

A plot of the beam pattern as a function of  $\theta$  is show in the Figure 4 for the electrostatic transducer series 600 of Polaroid Corp used in this work. From the beam pattern it can be confirmed that emission power decreases 3dB for an azimuth of about  $5.4^\circ$ , which defines  $11^\circ$  for the beamwidth. Within this angle the energy transmitted will eventually be enough for detecting its echo, after a favorable reflection.

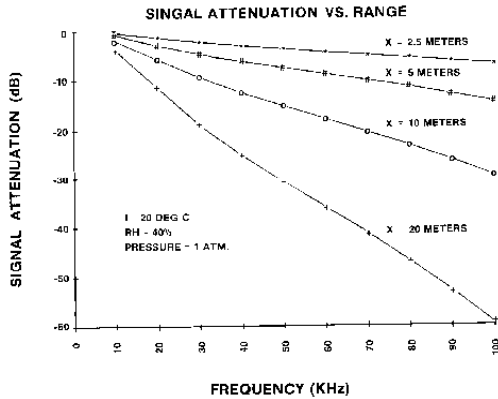


Figure 3. Beamwidth/Frequency/Radius

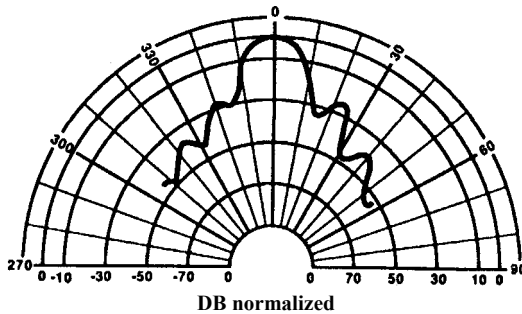


Figure 4. Beam pattern for the electrostatic transducer series 600 of Polaroid Corp. with the following parameters:  $c = 343.2$  m/s;  $a = 19$  mm and  $f = 50$  kHz

In summary, a single broadband transducer can be used adjusting the system beamwidth by setting the operating frequency according to the demands of the task. This will have additional effects on the transducer performance, since the way the sound is transmitted through the air is also frequency dependent: as the frequency increases the beamwidth decreases. However the maximum range will be decreased due to increased energy absorption.

### 3. Sonar sensors models

In the simplest model for sonar sensors the range measurement is interpreted as the distance to the nearest obstacle in the direction of the beam centerline. This model present several problems. Firstly, it fails for specular surfaces, which reflect sonar beam like a mirror. Furthermore a direct return is only produced from specular surfaces if the sonar beam is incident close to  $90^\circ$ . Secondly, for oblique incidence angles, either no return is produced, or a multiple specular reflection occurs originating wrong measurements. Finally, another problem with this model is that it ignores the width of the sonar beam not taking in consideration that the objects in the beam periphery may cause the reflections that come back to the sensor.

Elfes [1] build a navigation map based in a grid where each region was classified as empty, occupied, and unknown. Each sonar range measurement is interpreted as

providing information about “probably empty”, “somewhere occupied” volumes in the space, subtended by the beam sonar (a  $30^\circ$  opening angle in this case). The occupancy information is modeled by probability profiles. This model didn’t have into consideration the specularity. It produces good sonar maps in non-specular environments, but it can fail completely when the environment is specular.

Kuc and Siegel [5] made a model for the ultrasonic sensors based on the principles of acoustics and the knowledge of the detection circuitry of the Polaroid Range Finder, to find the reflections from corners, edges and walls. The main conclusion obtained from this model is that, for small incidence angles ( $<6^\circ$ ), the wave reflected from a specular wall will always measure the normal distance to the wall, independent of incidence angle. The model does not deal with effects caused by the irregular angular radiation pattern of the sonar transducer, and does not attempt to model non-specular surfaces.

Leonard and Durrant-Whyte [4] made a good description of the effects caused by the angular irregularity. They collect and plot several sets of range readings from specular surfaces, starting with a small increment in the incidence angle ( $0.588^\circ$ ) until a maximum angle of  $30^\circ$  is reached. For small incidence angles, where the beam intensity is strong, they found sequences of adjacent readings that define horizontally segment line. Those sequences were denominated “regions of constant depth-RCD”, which corresponds to arcs in Cartesian coordinates. The extraction of these regions is based on the difference between the minimum and the maximum values of a sequence of readings, inferior to a preset limit ( $|V_{\max} - V_{\min}| < \delta_r$ ). The width  $\beta$  of a RCD is the difference between the leftmost and rightmost angle of the readings. It is set a minimum value for  $\beta$ , usually between  $5^\circ$  and  $10^\circ$ . This value allows the distinction between “strong returns” and “weak returns”: if  $\beta < \beta_{\min}$  it is considered a weak return; if  $\beta \geq \beta_{\min}$  it is considered a strong return. Leonard and Durrant-Whyte stated that weak returns are caused by low intensity radiation in the beam’s side-lobes, and give a theoretical explanation for the overestimates, based on the properties of the Polaroid detection system. They propose that the best way to deal with weak returns is to ignore them. They also pointed out a method, based on searching for regions of constant depth, to distinguish weak from strong returns, and only to process the strong returns in their mapping system.

Harris and Recce in [3] describe a model for ultrasonic sensors based on analysis of a great group of data obtained with a Polaroid sonar. The collection of data is acquired starting from a fixed position with an angular spacing of  $1.8^\circ$ . They defined two models: one for rough surfaces and one for smooth surfaces. In the first case, the model allows to obtain the average  $\mu$  and the deviation  $\sigma$

of the readings acquired, as a function of the normal distance  $\delta$  and the incidence angle  $\theta_b$ . In the second case the model is based on a group of controlled values, with one input - the incidence angle - and three outputs: the direction probability of the return wave, the estimate of the average of the direct returns (average of the direct returns less the distance in the direction of the normal) and the deviation of the direct returns.

## 4. Implementation and results

### 4.1. Hardware configuration

The work cell used is composed by the following elements (Figure 5): a PUMA 560 manipulator used to position the sensors mounted on the wrist of the robot in order to acquire the surface profile; a controller area network (CAN) used for data acquisition and some basic control; a video camera mounted in the shoulder of the manipulator to define the work area, and the ultrasonic sensors mounted in the wrist to get the surface profile. The PUMA 560 is used as a scanner where the ultrasonic sensors acquire data for internal representation of the of the part's surface geometry. The ultrasonic sensors setup relative to the robot grip axis, is a square as presented in the figure 5. For this reason, it is only possible to acquire information relative to surfaces with square or rectangular shapes, because only in these cases it is possible to divide each part of the surface in smaller areas of identical shape. The maximum size of these areas depends on the setup and the diameter of the sonar sensors.

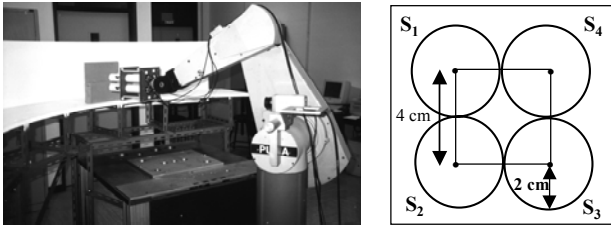


Figure 5. Work cell

The sensors used in this work are made by Polaroid Ultrasonic Ranging Units, which have a range of about 0.35 m to 10 m when the emission frequency is 52 kHz. A specific kit provided by Polaroid Corp controls the ultrasonic transducers. This kit is based on the Intel 80C196 microprocessor and is easy to configure by software. It is possible to configure the following parameters: transmission frequency, pulse width, blanking time, amplifier gain, sample rate and trigger source (internal/external). This kit is connected to the external world via RS-232. An analogue output proportional to the measured distance is also available. To avoid any eventual interference from the emission and echo waves, the sensors are triggered sequentially, leaving just one unit emitting at a time.

This configuration was only used for testing purposes but could also adapted for several applications, namely, pistol spray painting and glue application.

### 4.2. Strategies to minimize ultrasonic sensors limitations

With the goal of minimizing the problems caused by the sonar sensors limitations mentioned before and taking into consideration the proposed hardware, the following options were made:

1. A tube with about 20 cm was placed in front of each sensor (Figure 6);
2. The operating frequency was increased from 50 kHz to 63 kHz;
3. 8 pulses instead of 16 were used and the blanking time was decreased from 2.38 ms to 1.38 ms;
4. The global and exponential gains as well as the minimum limit for the detection were properly echo adjusted (within the electronic module).

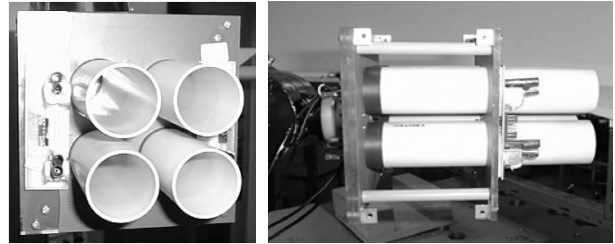


Figure 6. Detail of the sonars in the wrist

The main objective of options 1. and 2. is to reduce the opening angle value in order to increase the directionality in the intended operating range. The operating frequency increase also improves the angular resolution but, on the other hand, there is a greater attenuation of the transmitted wave and a decrease in the value of the maximum measurable distance. This attenuation doesn't cause any problem in referred kind of applications, because the maximum value to measure never exceeds 80 cm, while the maximum value measured with this configuration can go up to approximately 2 m (value obtained in practice).

With option 3. the minimum measurable distance could be reduced from 40 cm to 25 cm. In addition the opening angle is also reduced for the same operating range and the resolution is increased. As a result of the procedure suggested in point 3. the sample time could also be increased.

Finally, the procedure described in 4. guaranties that the echo is properly received within the intended measuring range and that noise (acoustic and electric) is minimized.

### 4.3. Acquiring the empirical sonar model

The object used in the tests is shown in Figure 7. The robot locates one sonar sensor pointing to the locations (1, 2 and 3) in the object surface. The distance between the sensor and the surface is about 40 cm and the wave

emitted is approximately perpendicular to the surface (the incidence angle  $\alpha$  is less than  $8^\circ$ ). For each location 50 measurements were taken.

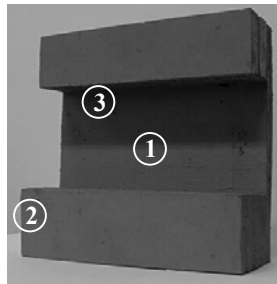


Figure 7. Object used in the tests

The results obtained were the following:

**Point 1**

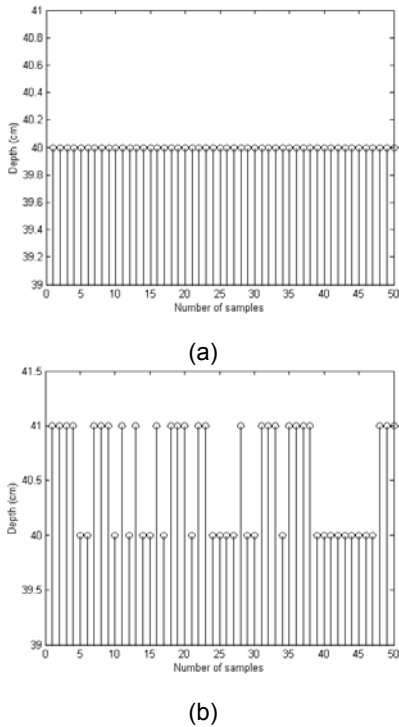


Figure 8: Sonar data in location 1: (a) with a incidence angle equal to zero ( $\alpha = 0^\circ$ ); (b) with a incidence angle close to  $8^\circ$

**Point 2**

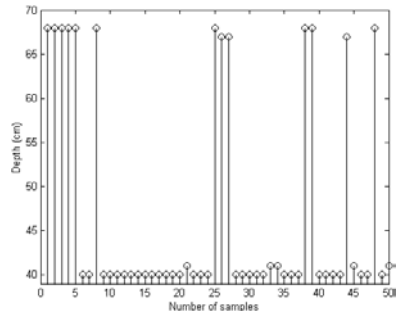


Figure 9. Sonar data in location 2

**Point 3**

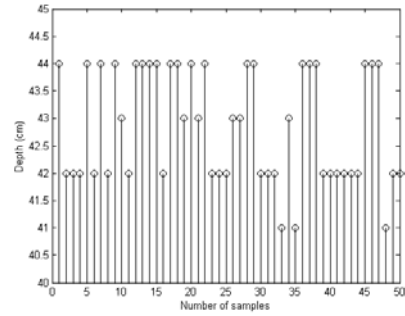


Figure 10. Sonar data in location 3

The first conclusion of these tests confirms the results of previous works, that is, for small incidence angles ( $\alpha < 8^\circ$ ) the probability of obtaining a direct return is maximum. On the other hand, it was sometimes observed that the values obtained from the ultrasonic sensor with a fixed position had an oscillation more or less important. For the purpose of this work it is important to clarify this problem because it is necessary to acquire the profile of the surface with minimum error. Three different tests were performed with the sonar sensor fixed in a position and pointing to the different locations. The tests were the following: 1) starting with the beam perpendicular to the surface (location 1 in Figure 7) the incidence angle was increased to a maximum of approximately  $8^\circ$ ; 2) with the beam perpendicular to the surface but pointing to the location on the edge of the object (location 2 in Figure 7; 3) with the beam perpendicular to the surface of the model but pointing to a zone of depth transition (location 3 in Figure 7).

The measurement variations shown in Figure 8 (b) are not significant, because they are essentially due to the rounding up of the calculations of the distance. In this case, it can be considered that for angles smaller than  $8^\circ$  the values obtained practically don't have any fluctuation ( $\leq 1$  cm). In Figure 9, the highest values (68 cm) correspond to the distance to the bottom of the table where the object is positioned and the other measurements correspond to the real distance to the object. In figure 10 the observed variations are due to small reflections caused by the proximity of zones with relevant different depths.

From the analysis of the obtained data two new concepts were defined: Points of Constant Depth (PCD) and Areas of Constant Depth (ACD). The PCD are points that represent a small area, which is related with the diameter of the ultrasonic sensor and with the opening angle of the respective beam. This point corresponds to a spot on the surface where the angle between the line of emission and the surface of the measured object is  $90^\circ$ . The ACD are square regions with a maximum side of 4 cm, value imposed by the distance between the centers of the ultrasonic sensors. However, it is possible to define smaller area ACD's. The shape of the ACD area can be a

square or rectangle depending on the layout of the ultrasonic sensors on the robot's wrist.

**4.3.1. Points of Constant Depth (PCD).** A data vector acquired from the four sonar sensors in a fixed position defines a point of constant depth when the difference between the maximum value and the mean of the vector is smaller than a threshold ( $\delta$ ) defined beforehand. If

$$MAX_{Data\ vector} - \bar{x}_{Data\ vector} < \delta \Rightarrow \text{PCD}$$

With

$$\bar{x}_{Data\ vector} = \frac{1}{n} \sum_{j=1}^n x_j \quad n - \text{Number of elements of the}$$

data vector

In the case of this application the  $\delta$  used it is set to 1 cm and the distance set to PCD is the average of the data vector.

The PCD definition allows the distinction between the strong and weak returns. Only the strong returns are processed and solely these can define a PCD.

**4.3.2. Areas of Constant Depth (ACD).** The extraction of areas of constant depth is based on PCDs. In this case four PCDs are always used, corresponding to the four sonars located in the wrist of the robot.

A certain area constitutes an ACD when the difference in absolute value between the averages of PCDs (making all the possible combinations) doesn't exceed a predefined limit. If the following condition,

$$\left| \bar{x}_{sensor1} - \bar{x}_{sensor2} \right| < \delta_R \quad \text{e} \quad \left| \bar{x}_{sensor1} - \bar{x}_{sensor3} \right| < \delta_R \quad \text{e} \\ \left| \bar{x}_{sensor1} - \bar{x}_{sensor4} \right| < \delta_R \quad \text{e} \quad \left| \bar{x}_{sensor2} - \bar{x}_{sensor3} \right| < \delta_R \quad \dots$$

is true, then the PCD's define a ACD, whose depth is equal to the average of the averages of PCDs:

$$\bar{x}_{ACD} = \frac{1}{n_{PCD}} \sum_{j=1}^{n_{PCD}} \bar{x}_{j(PCD)} \quad n_{PCD} - \text{Number of PCDs.}$$

In this case the  $\delta_R$  was set to 1.5 cm, a value determined through experimental tests.

If a set of PCDs cannot define an ACD, another search for a new set of PCD's is done using the following interactive procedure: two PCDs are kept while a search for two new PPCs is done incrementing the robot arm position.

## 5. Conclusions

A sensorial system based in sonar sensors was built to acquire the profile of surfaces with the minimum error. In order to minimize the measurement error resulting from

the beam opening angle, the sensors were covered with a tube with a length of 20 cm and the operating frequency was increased. Together with this a new empirical model for sonar sensors was defined, based on two concepts: the PCD and ACD.

One of the purposes of this paper is to try to demystify the poor image of sonar sensors and show that in spite of some limitations they also present potentialities that when well explored allow their use in many applications, both in mobile and static robotics.

In mobile robotics sonar sensors are not, typically, used alone - the data is usually complemented with inputs from sensors with a better directionality as, for instance, laser or infrared sensors. However, using available sonar systems with different operating frequencies and appropriated layouts, directionality and accuracy can be increased.

In the static robotics it is possible to acquire the profile of surfaces, when high accuracy is not needed, and generate the trajectories for different applications, for instance for painting to the pistol and application of glues. Another possibility is the application for object recognition. Data fusion/integration techniques can be used to further increase the measurements accuracy.

## 6. References

- [1] Alberto Elfes, "Sonar-Based Real-World Mapping and Navigation", *IEEE Journal of Robotics and Automation*, IEEE, Vol. RA-2 No. 3, June 1987, pp. 249-265.
- [2] Gerald D. Maslin, "A simple Ultrasonic Ranging System", *102<sup>nd</sup> Convention of the Audio Engineering Society at Cincinnati*, May 1983.
- [3] Kenneth D. Harris and Michael Recce, "Experimental modeling of time-of-flight sonar", *Robotics and Autonomous Systems*, Elsevier, No. 24, 1998, pp. 33-42
- [4] John J. Leonard, and Hugh F. Durrant-Whyte, *Directed Sonar Sensing for Mobile Robot Navigation*, Kluwer Academic Publishers, Chapter 2, 1992.
- [5] Roman Kuc, and M. W. Siegel, "Physically Based Simulation Model for Acoustic Sensor Robot Navigation", *IEEE Transactions on Pattern Analysis and Machine Intelligence*, IEEE, Vol. PAMI-9 No. 6, November 1987, pp. 766-778.